Could changing ocean circulation have destabilized methane hydrate at the Paleocene/Eocene boundary?

Karen L. Bice

Department of Geology and Geophysics, Woods Hole Oceanographic Institution, Woods Hole, Massachusetts, USA

Jochem Marotzke

School of Ocean and Earth Science, Southampton Oceanography Centre, Southampton, UK

Received 8 August 2001; revised 10 December 2001; accepted 8 January 2002; published 10 May 2002.

[1] During the Paleocene-Eocene Thermal Maximum (PETM, ~55 Ma), marine and terrestrial carbon isotope values exhibit a negative shift of at least 2.5‰, indicative of massive destabilization of marine methane hydrates, releasing ~2000 gigatons of methane carbon. The cause of the hydrate destabilization is unknown but has been speculated to be warming due to a change from high-latitude to low-latitude deepwater formation. Here we present results from a numerical ocean model indicating that a sudden switch of deepwater formation from southern to northern high latitudes caused middepth and deep-ocean warming of 3°–5°C. The switch is caused by a slow increase in the intensity of the atmospheric hydrologic cycle, as expected under increasing temperatures and consistent with PETM sedimentary evidence. Deepened subtropical subduction prior to the thermohaline circulation switch causes warming of 1°–4°C in limited areas at thermocline through upper intermediate depths, which could destabilize methane hydrates gradually and at progressively greater depths. Warming accompanying a south-to-north switch in deepwater formation would produce sufficient warming to destabilize seafloor gas hydrates over most of the world ocean to a water depth of at least 1900 m. *INDEX TERMS:* 1620 Global Change: Climate dynamics (3309); 3344 Meteorology and Atmospheric Dynamics: Paleoclimatology; 4255 Oceanography: General: Numerical modeling; 4267 Oceanography: General: Paleoceanography; *KEYWORDS:* paleoceanography, modeling, Paleocene, Eocene, methane, hydrology

1. Introduction

[2] Fifty-five million years ago, the Earth underwent an abrupt climate change known as the Paleocene-Eocene Thermal Maximum (PETM). Against the backdrop of an already warm climate with reduced pole-equator temperature contrasts, intermediate- to deep-ocean water temperatures and high-latitude surface temperatures increased by 6°–8°C over <20 kyr [*Röhl et al.*, 2000]. The PETM is characterized by a negative shift of 2.5‰ (Peedee belemnite (PDB)) or more in marine carbonate $\delta^{13}C$ records [*Kennett and Stott*, 1991; *Thomas and Shackleton*, 1996] and of >5‰ in terrestrial $\delta^{13}C$ records [*Koch et al.*, 1992]. A feasible explanation for the negative carbon isotope excursion at the PETM is the introduction of ~2000 gigatons of isotopically depleted (−60‰) carbon to the ocean-atmosphere system [*Dickens et al.*, 1995; *Dickens*, 2000, 2001; *Matsumoto*, 1995]. One possible source for this quantity of depleted carbon today is the vast reserves of natural gas hydrate in oceanic sediments and methane gas trapped beneath these deposits [*Kvenvolden*, 1998].

[3] The thermal forcing of the late Paleocene and early Eocene thermohaline circulation (THC) was reduced compared to today because the pole-equator temperature contrast was smaller. Therefore it has often been speculated that the oceans might have been characterized by deepwater formation at low latitudes as first suggested by *Chamberlin* [1906]. Abrupt bottom warming caused by the onset of or an abrupt increase in this putative low-latitude deepwater source has been invoked as a feature of the PETM [*Kennett and Stott*, 1991; *Kaiho et al.*, 1996; *Bains et al.*, 1999], but there has been no evidence from data or from model studies that deep water originated from low latitudes, rather than from warm high latitudes [*Crowley*, 1999; *Bice and Marotzke*, 2001]. Nonetheless, changing thermohaline circulation is perhaps the most likely mechanism for abrupt, global bottom water temperature change.

[4] *Zachos et al.* [1993] noted that the abrupt and brief PETM event may be integrally related to the gradual late Paleocene-early Eocene global warming trend itself. In other words, the PETM may have occurred because global climate was gradually warming and some climate system threshold was passed, causing the system to "jump" to a new equilibrium state. Such jumps between different stable equilibria have been noted in coupled models with Quaternary, modern, and hypothesized future boundary conditions, both with and without a forcing perturbation [e.g., *Manabe and Stouffer*, 1988, 1993, 1995; *Rahmstorf and Ganopolski*, 1999; *Hall and Stouffer*, 2001].

[5] The precise nature of such a threshold response in the latest Paleocene thermohaline circulation has not previously been identified. Here we show new ocean model results suggesting that an abrupt switch in deep convection from high southern to high northern latitudes could be caused by a gradual strengthening of the idealized atmospheric hydrologic cycle, a change consistent with a gradually warming climate [*Manabe*, 1996] and PETM sedimentary evidence [*Robert and Kennett*, 1994; *Schmitz et al.*, 2001].

2. Ocean Model Experiments

[6] *Bice and Marotzke* [2001] describe uncoupled Paleogene ocean model experiments using mixed boundary conditions and atmospheric forcings consistent with peak PETM warming. They examine the sensitivity of the model to imposed water cycle perturbations and the parameterizations of continental runoff and ocean diapycnal mixing for one early Eocene paleogeographic reconstruction. In this study, we first repeat the moisture flux experiment of Bice and Marotzke but with atmospheric surface forcings representative of pre-PETM conditions. We then examine

0883-8305/02/2001PA000678$12.00

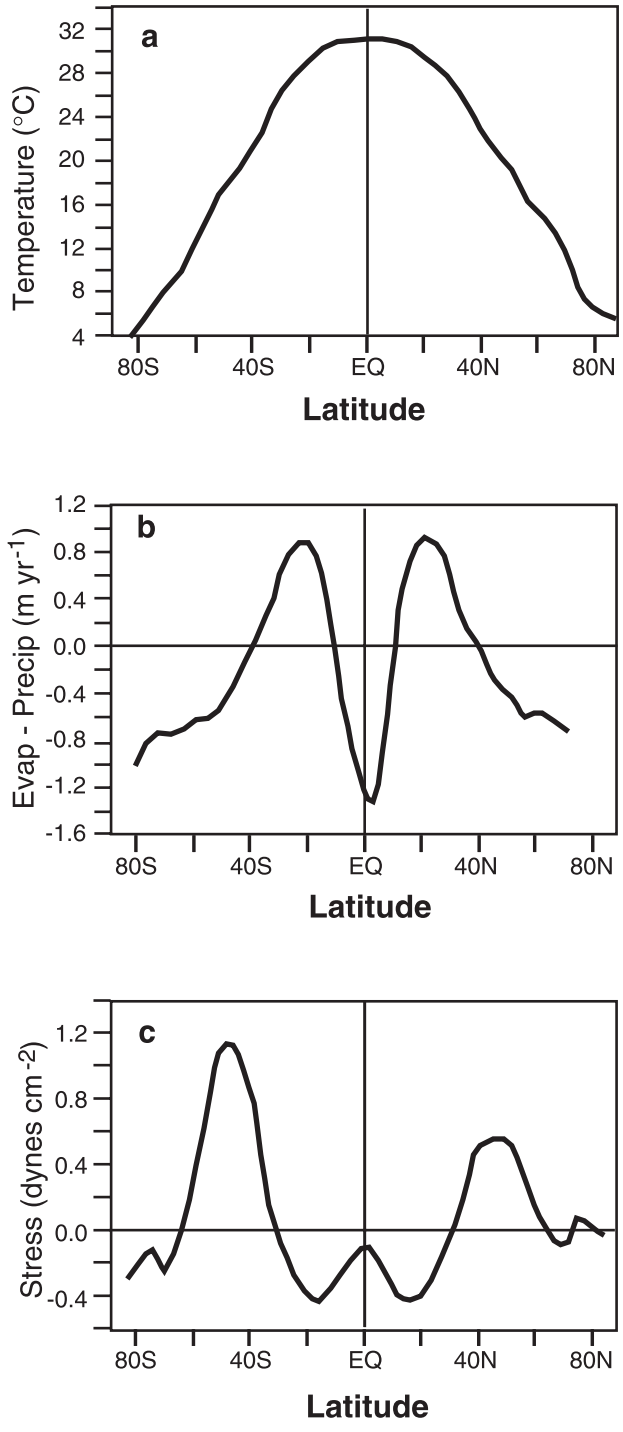

Figure 1. (a) Temperature, (b) evaporation minus precipitation rate for the control case, and (c) zonal wind stress forcings from the atmospheric model.

the sensitivity of the model response to plausible changes in paleogeography around the time of the Paleocene-Eocene boundary.

2.1. Model Description

[7] The model and forcing technique are the same as those used by *Bice and Marotzke* [2001]. The ocean model is the Geophysical Fluid Dynamics Laboratory's Modular Ocean Model (MOM), version 2.2 [*Pacanowski*, 1996]. The ocean surface is forced using "mixed thermohaline surface boundary conditions" [e.g., *Bryan*, 1986] of zonally invariant temperature, wind stress, and moisture fluxes (evaporation rate minus precipitation rate, $E-P$) predicted by an atmospheric general circulation model (AGCM), GENESIS, version 2.0 [*Thompson and Pollard*, 1997] (Figure 1). The AGCM atmospheric composition (CO_2 = 645 ppmv; CH_4 = 16.5 ppmv) and poleward heat parameterization (4 times the modern control value) were set in order to produce a qualitatively good match to estimates of latest Paleocene high-latitude sea surface temperatures. The AGCM yields an ocean surface temperature of 11°C at paleolatitude 63°S, a value within the uncertainty in the 13°–14°C estimate from the planktonic foraminifera *Acarinina* at Ocean Drilling Program (ODP) Site 690 below the PETM [*Stott et al.*, 1990; *Thomas and Shackleton*, 1996]. It should be noted that although widely used in paleoclimate studies, the standard approach of matching model and planktonic isotopic temperatures by varying greenhouse gas concentrations and other parameters in the AGCM is not an exact science: more than one combination of CO_2, CH_4, and heat transport coefficients could produce a reasonable fit to reconstructed sea surface temperatures. Because of the large number of model runs required to perform the single variable sensitivity experiments described here it is impractical to also test the ocean model sensitivity to hydrologic cycle increases under other, slightly different combinations of AGCM parameters.

[8] The initial paleogeographic configuration used is the same as that used by *Bice and Marotzke* [2001], based on an early Eocene reconstruction by Chris Scotese [*Bice et al.*, 2000a] (Figure 2). Paleobathymetry is based on seafloor age-depth relationship as described by *Bice et al.* [1998]. Important paleogeography sensitivity tests are described below. A detailed discussion of the modeling approach, its limitations, and further sensitivity tests are given by *Bice and Marotzke* [2001].

2.2. Water Cycle Perturbation Experiments

[9] The suite of dramatic global changes inferred for the PETM includes increased aridity in subtropical latitudes and increased high-latitude precipitation [*Robert and Kennett*, 1994; *Schmitz et al.*, 2001]. This pattern is consistent with an increase in the intensity of the global hydrologic cycle, which would be expected with increasing atmospheric CO_2 concentration, a change that might have accompanied late Paleocene volcanism [*Eldholm and Thomas*, 1993; *Bralower et al.*, 1997]. The reader is referred to an excellent nontechnical description of intensification of the water cycle by *Manabe* [1996], but the fundamental features of the hydrologic cycle response to an increase in the atmospheric concentration of carbon dioxide are these: (1) the global mean evaporative flux (or rate of water transfer between the ocean and atmosphere) increases with increased net downward flux of radiation and surface warming, (2) increased mean evaporation rate is balanced by increased precipitation rate, (3) evaporation rate increases more in the subtropics than at other latitudes, and (4) increased precipitation exceeds increased evaporation at high latitudes, an effect enhanced by increased poleward transport of moisture due to tropospheric warming [*Manabe*, 1996]. In general, then, the hydrologic cycle response to increased atmospheric carbon dioxide concentration is represented by increased subtropical evaporation and increased high-latitude precipitation [*Manabe and Bryan*, 1985; *Manabe*, 1996].

[10] In order to examine the possible ocean response to a gradual increase in the strength of the water cycle alone, the ocean is forced first with the moisture flux ($E-P$) predicted by the AGCM. The moisture flux is then multiplied, uniformly, by factors increasing from 1.0 to 2.0 in steps of 0.1 every 500 years, producing higher evaporative fluxes in the subtropics and higher net precipitation at high latitudes while

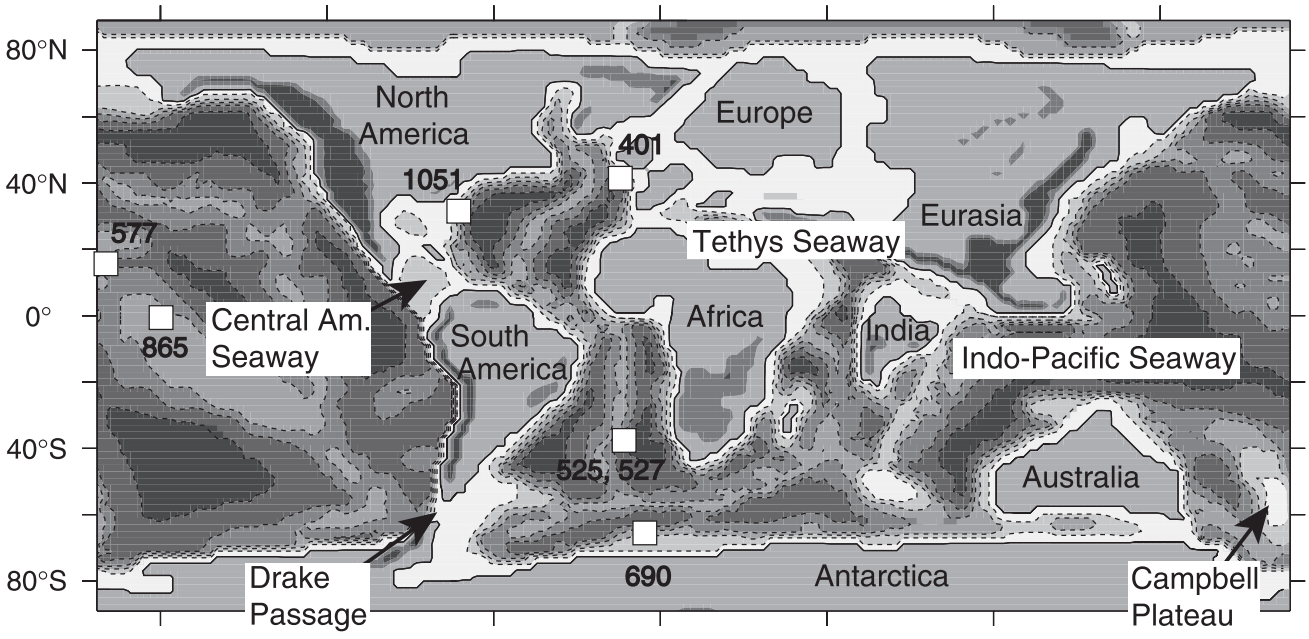

Figure 2. Baseline paleogeography at 2° resolution. Solid curve indicates the shoreline; dashed contours indicate ocean depths of 1, 2, 3, 4, and 5 km. Deep Sea Drilling Program (DSDP) and Ocean Drilling Program (ODP) sites mentioned in the text are shown.

maintaining a net zero surface flux. In all runs, temperature and wind stress forcing are identical. This imposed perturbation of $E-P$ represents the increase in water cycle simulated in coupled models with increased atmospheric CO_2 [*Manabe*, 1996]. Thus the uncoupled ocean model used here parameterizes one of the most important changes of the coupled system, albeit in a relatively crude form.

[11] Forced by the (unperturbed) moisture flux predicted by the AGCM, the global circulation is very similar to the control run of *Bice and Marotzke* [2001], despite cooler polar temperatures, a greater pole-equator temperature gradient, and stronger zonal wind stresses. Deep water is formed in a broad region of the Southern Hemisphere along the Antarctic margin between Australia and the Antarctic Peninsula. This bottom water is carried west and northward along bottom topography east of Australia. It flows westward along the New Guinea margin into the eastern Indian Ocean and is turned southward around Ninetyeast Ridge, Broken Ridge, and Kerguelen Plateau, which had paleodepths as shallow as 500–1500 m in the early Paleogene [*Driscoll et al.*, 1989; *Peirce et al.*, 1989; *Quilty*, 1992]. Some deep water circulates northward into the deep western Indian Ocean. Deep water is prevented by topography from flowing directly into the deep Atlantic basins. Instead, it mixes with intermediate water across topography in the Southern Ocean, at Walvis Ridge and in the Equatorial Fracture Zone to fill these deep, silled basins from the south. In the North Pacific an intermediate (to 1500 m) water mass forms near the Alaskan margin and flows southwestward along the Asian margin. Much of this water is recirculated in the interior of the North Pacific basin; a smaller amount mixes with Southern Ocean water north of New Guinea to contribute to eastern Indian Ocean water.

[12] Forced by the imposed $E-P$ perturbation, as described above, thermohaline circulation changes little, but the global ocean temperature increases gradually by ~1°C (black curve in Figure 3), with maximum warming (up to 7°C) occurring at between 400 and 1200 m in the subtropical North Atlantic. As discussed in detail by *Bice and Marotzke* [2001], this warming is the result of deepened subduction. Subduction is the process by which warm, relatively saline, subtropical surface waters are moved downward and spread horizontally along isopycnal (equal density) surfaces into the main thermocline [*Luyten et al.*, 1983; *Price*, 2001]. As the $E-P$ factor increases, subtropical surface salinity increases (<1 psu) cause subduction to carry subtropical water to greater depth, warming the thermocline. This response suggests deepened subduction as a plausible mechanism for midwater warming and consequent limited methane release, but the magnitude of the subduction-induced

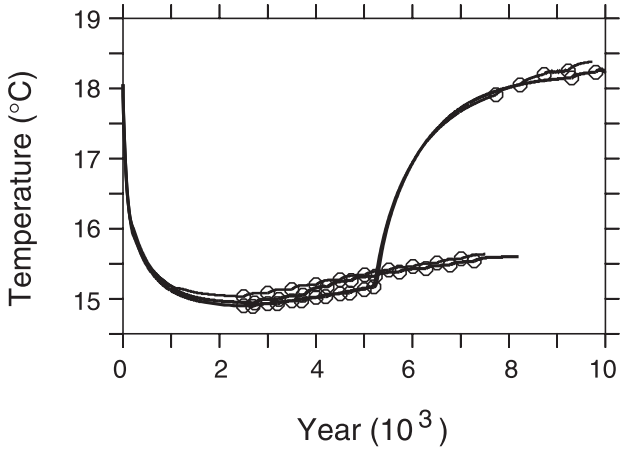

Figure 3. Time series of global mean ocean temperature for the four paleogeography sensitivity tests. The circles indicate the points at which the $E-P$ forcing to the ocean model was increased by 10%. Temperature and wind stress forcings were held constant throughout. Colors indicate the following cases: black, open North Atlantic, open India-Eurasia gateway (Figures 4a and 4c); blue, open North Atlantic, closed India-Eurasia gateway (Figures 4a and 4d); green, Brito-Arctic bridge, closed India-Eurasia gateway (Figures 4b and 4d); red, Brito-Arctic bridge, open India-Eurasia gateway (Figures 4b and 4c). See color version of this figure at back of this issue.

Table 1. Comparison of Temperatures Inferred From $\delta^{18}O$ of Benthic Foraminifera Across the PETM and Those Predicted by the Ocean Model[a]

Site	Estimated Water Paleodepth, m	Pre-PETM and PETM Sample Depths, mbsf	Pre-PETM and PETM $\delta^{18}O$, ‰ PDB	Pre-PETM to PETM °T (°C) From Isotopes	Maximum °T Response to Subduction	Mean °T (°C) Response to THC Switch
401	1800	202.60, 202.00	0.11, −0.54[b]	2.9	1.1	3.6
525	1600	392.81, 392.41	0.03, −1.50[c]	6.9	0.9	3.6
527	3400	201.07, 200.89	−0.32, −1.35[c]	4.7	0.4	4.4
577	1950	82.03, 81.94	−0.32, −0.98[d]	3.0	0.5	4.2
690	1900	170.65, 170.42	−0.18, −1.17[e]	4.5	0.4	4.4
865	1400	103.00, 102.96	0.0, −1.16[f]; 0.15, −1.09[g]	5.2; 5.6	0.6	4.0
1051	2000	512.82, 512.73	0.28, −1.22[h]	6.7	0.3	3.2

[a] The isotopic temperature calculation [*Erez and Luz*, 1983] assumes local bottom water $\delta^{18}O$ equaled −1‰ (SMOW) and did not change across the PETM.
[b] *Cibicidoides* [*Pak and Miller*, 1992]. The peak PETM is missing in benthic records from Site 401, so the Δδ recorded here is an underestimate of the actual change.
[c] *Nuttallides* [*Thomas and Shackleton*, 1996].
[d] *Nuttallides* [*Pak and Miller*, 1992]. Samples across the P/E boundary at Site 577 do not contain the PETM. The Δδ recorded here is for pre-PETM to post-PETM specimens.
[e] *Bulimina ovula* [*Thomas and Shackleton*, 1996; *Thomas et al.*, 2000].
[f] *Cibicidoides* [*Zachos et al.*, 2001].
[g] *Bulimina ovula* [*Zachos et al.*, 2001].
[h] *Oridorsalis* [*Katz et al.*, 1999]. The onset of the PETM is missing in Site 1051, but peak PETM values appear to have been recorded. Depth from *Katz et al.* [2001].

warming is too small by itself to account for PETM bottom water warming at sites with intermediate paleodepths (Table 1).

2.3. Paleogeographic Sensitivity Experiments

[13] We now examine the sensitivity of the ocean response to this same hydrologic cycle increase taking into consideration uncertainty in the precise paleogeographic reconstruction. The moisture flux perturbation experiment is repeated with three additional global ocean configurations, specifying either or both of the following changes: (1) North Atlantic basin modified to represent uplift and island construction associated with North Atlantic Volcanic Province magmatism and heat flow (Figures 4a and 4b)

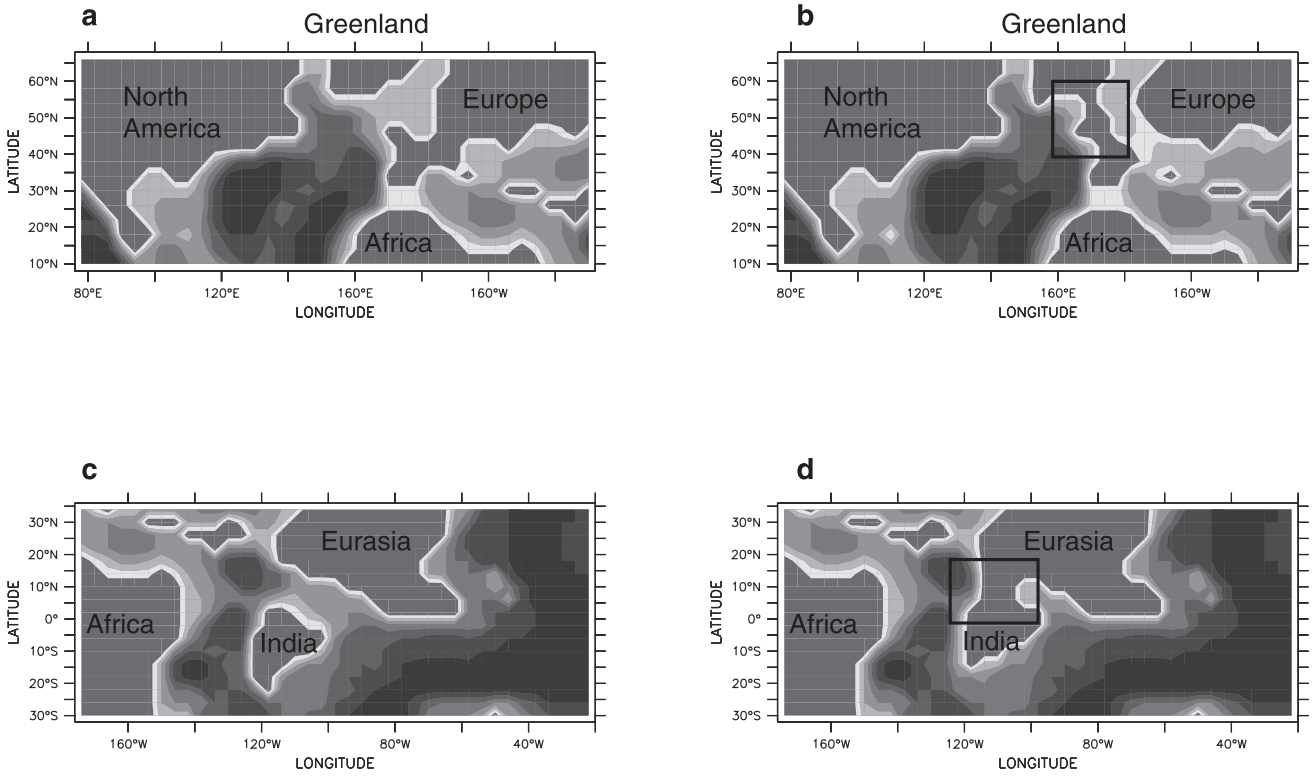

Figure 4. Maps showing regional paleogeographies examined in ocean model sensitivity experiments. (a) Open North Atlantic, (b) Brito-Arctic bridge in the North Atlantic basin, (c) open India-Eurasia gateway, (d) closed India-Eurasia gateway. Gray, land; purple and blues, ocean shallower than 1500 m; orange and reds, ocean deeper than 3000 m. See color version of this figure at back of this issue.

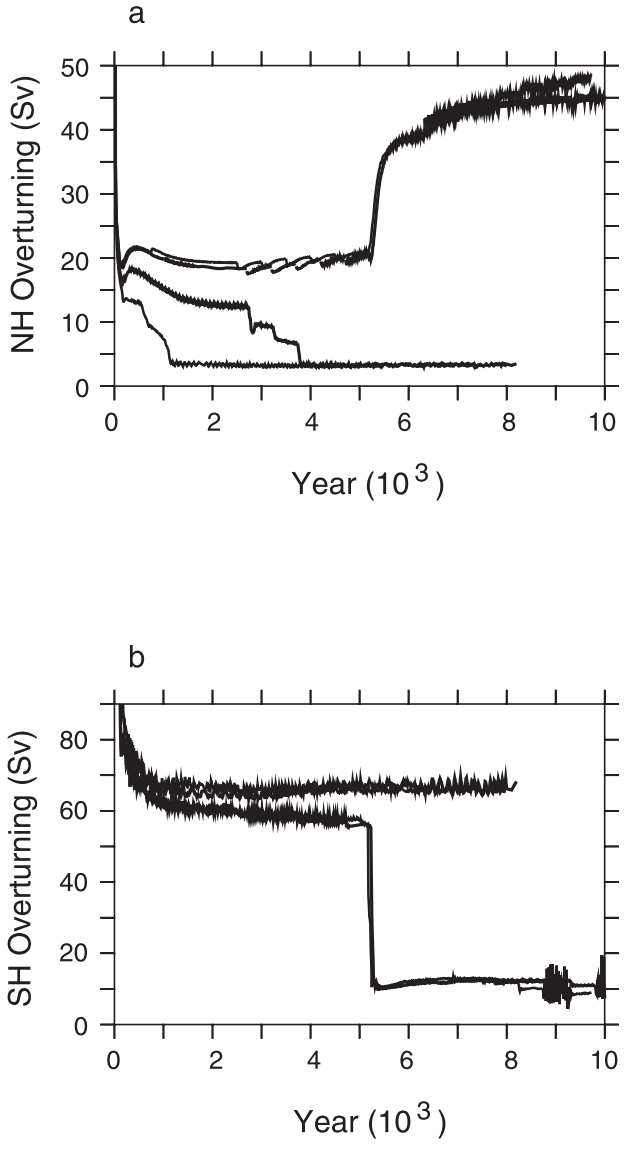

Figure 5. Time series of the maximum meridional overturning strength (Sverdrups) for (a) Northern Hemisphere and (b) Southern Hemisphere. Colors are as indicated for Figure 3. See color version of this figure at back of this issue.

and (2) closed low-latitude gateway with the earliest collision of western India and Eurasia (Figures 4c and 4d). These changes represent plausible geographic configurations during the late Paleocene-early Eocene interval [*Eldholm and Thomas*, 1993; *Ritchie and Hitchen*, 1996; *Beck et al.*, 1998; *Knox*, 1998; *de Sigoyer et al.*, 2000; *Clift et al.*, 2002]. Of particular relevance to these experiments is evidence that extensive subaerial volcanism existed in the late Paleocene in the North Atlantic [*Roberts et al.*, 1984; *Boulter and Manum*, 1989; *Clift et al.*, 1995; *White and Lovell*, 1997]. *Clift and Turner* [1998] describe evidence (including coal deposits) of subaerial exposure in the latest Paleocene in the Greenland-Iceland-Faeroe Ridge region. Substantial relative sea level fall in the North Sea at the PETM due to high heat flow also supports the plausibility of a significant barrier to ocean flow in the North Atlantic region [*Knox*, 1998]. Additionally, there is evidence to support the existence of a North Atlantic land bridge as a high latitude corridor for mammal migration from Europe to North America via Greenland at the Paleocene-Eocene boundary [*Knox*, 1998; *Tiffney*, 2001]. In fact, the appearance of many mammal orders in North America by migration across this bridge and a possible Bering land bridge occurs precisely coincident with the terrestrial record of the PETM [*Koch et al.*, 1995; *Maas et al.*, 1995; *Clyde and Gingerich*, 1998]. We will use the shorthand "Brito-Arctic bridge" to refer to a plausible barrier to flow in the North Sea region associated with magmatism and high heat flow activity of the Iceland Plume in the latest Paleocene.

[14] Forced by the imposed $E-P$ perturbation, all three paleogeographic sensitivity experiments exhibit thermocline and upper intermediate water warming due to deepened subduction. However, when a Brito-Arctic bridge is specified in the North Atlantic basin, with India-Eurasia either open or closed, the THC undergoes an abrupt switch from dominant Southern Hemisphere sinking to Northern Hemisphere (Pacific) sinking at a factor of 1.6 ($E-P$). Northern Hemisphere overturning increases abruptly from 20 to 45 Sv (1 Sv = 10^6 m^3/s)(Figure 5a), with what had been intermediate depth convection near the Alaskan margin deepening abruptly to 5200 m. Bottom water formation abruptly decreases along the Antarctic margin region, but intermediate depth ($\sim$1200 m) convection continues in a small area to the west of the Antarctic Peninsula. Southern hemisphere THC strength decreases from 60 to 12 Sv (Figure 5b). This switch in THC produces 3°–5°C warming in the deep ocean. Prior to the switch, 11°–12°C surface water convected at 74°–80°S in the Pacific sector Southern Ocean. Bottom water warming occurs with the switch to convection of 15°–16°C surface water at $\sim$66°N on the Alaskan margin. The global mean ocean temperature increases by $\sim$3°C over several thousand years.

[15] The abrupt switch in THC occurs because North Pacific upper ocean salinities gradually increase, despite the fact that the stronger atmospheric water cycle causes more net precipitation at high latitudes. The primary mechanism for maintaining high surface salinities in the northern North Pacific is increased transport of saline subtropical North Atlantic thermocline water through the Central American Seaway into the North Pacific basin. With the creation of a Brito-Arctic bridge, low-salinity North Sea water, which otherwise was introduced directly into the North Atlantic, is instead diverted south and eastward into the northern Tethyan basin. This allows moderately higher salinity water to develop in the North Atlantic subtropics, which is transported southward and westward into the Pacific. There much of it is entrained in the subtropical gyre and transported to the high-latitude North Pacific.

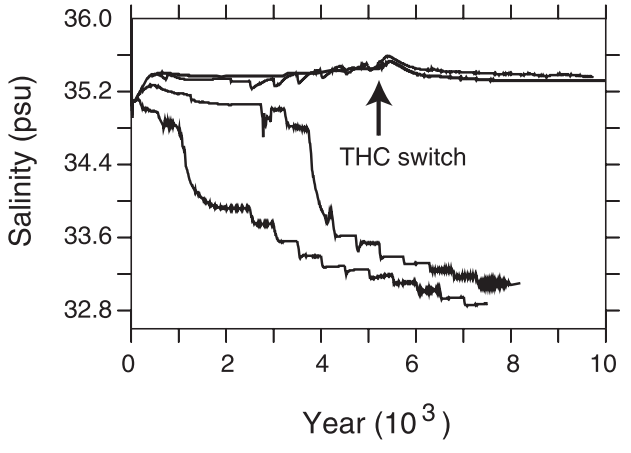

Figure 6. Time series of North Pacific upper ocean salinities in the region of convection, near the Alaskan margin. Colors are as indicated for Figure 3. See color version of this figure at back of this issue.

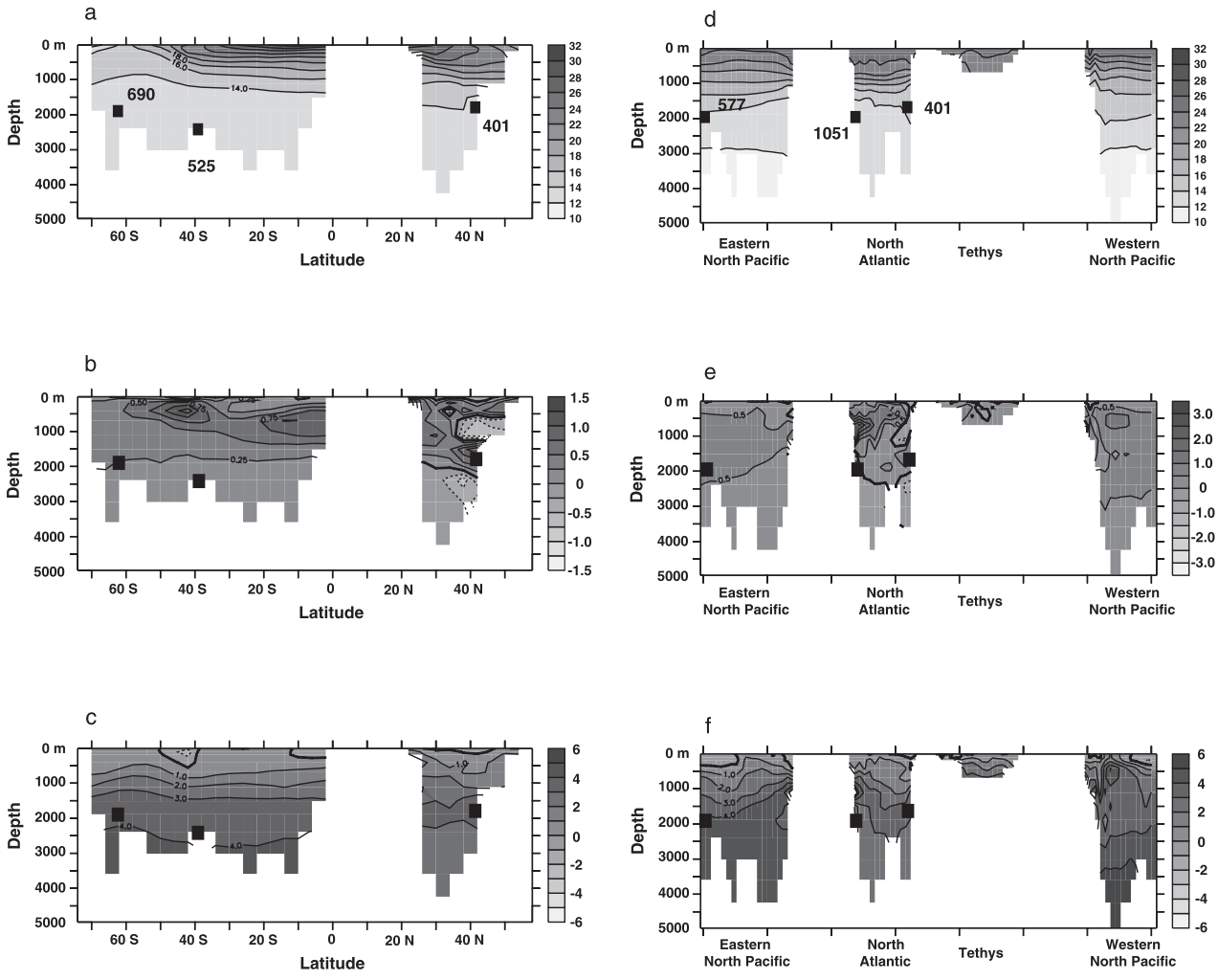

Figure 7. (a–c) Meridional cross sections through the Atlantic basins at the longitude of DSDP Site 401. (d–f) Zonal cross sections near the paleolatitude of Site 401 (38°N). Temperatures from the control case are shown in Figures 7a and 7d. Temperature differences due to deepened subduction are shown in Figures 7b and 7e. Temperature differences due to the THC switch are shown in Figures 7c and 7f. Positive values (reds) indicate warming caused by deepened subduction or by the switch from Southern to Northern Hemisphere bottom water formation. See color version of this figure at back of this issue.

The intermediate water sinking in the Northern Hemisphere is therefore not diminished as $E-P$ increases from 1.0 to 1.5 ($E-P$). It is instead maintained, and North Pacific salinity slowly increases, by <0.2 psu (Figure 6), until finally a switch to Northern Hemisphere sinking occurs at a 60% increase in $E-P$. Bottom water then forms in the North Pacific and fills the deep basins north and east of the Emperor-Hawaiian seamount chain and topography associated with the Pacific Superswell. It also flows west and southwestward as a deep Asian boundary current and turns westward through the Indonesian passage into the eastern Indian Ocean basin.

3. Model-Data Temperature Comparisons

[16] The unperturbed (pre-PETM) temperatures and predicted temperature change are shown in Figure 7 for two north-south and west-east vertical sections through all ocean basins. Figures 7a and 7d show the model-predicted temperatures for the control $E-P$ case (pre-PETM). Nearby deep sea sites from which benthic paleotemperature estimates are available (Table 1) are projected onto the sections. Figures 7b and 7e illustrate the warming between the control $E-P$ case and 1.5 $E-P$, just prior to the THC switch. Figures 7c and 7f show the temperature difference between the control $E-P$ case and 1.6 $E-P$, after the THC switch has occurred and the ocean model has approached a new steady state.

[17] One way to assess the validity of the predicted THC switch at the P/E boundary is to compare the model-predicted bottom water temperatures and temperature change against pre-PETM and PETM benthic foraminiferal oxygen isotope data. Unfortunately, there are very few localities from which both pre-PETM and peak PETM data are available, a result primarily of widespread dissolution of carbonate and hiatuses at the PETM [*Thomas*, 1998]. At those sites where sufficient carbonate material remains to allow recognition of the carbon isotope event, the size of the PETM excursion as expressed in the geochemistry of foraminifera is often truncated, allowing only a minimum temperature change to be inferred from $\delta^{18}O$. The sites from which benthic foraminiferal $\delta^{18}O$ measurements of pre-PETM and PETM (or immediately post-PETM) specimens are known are

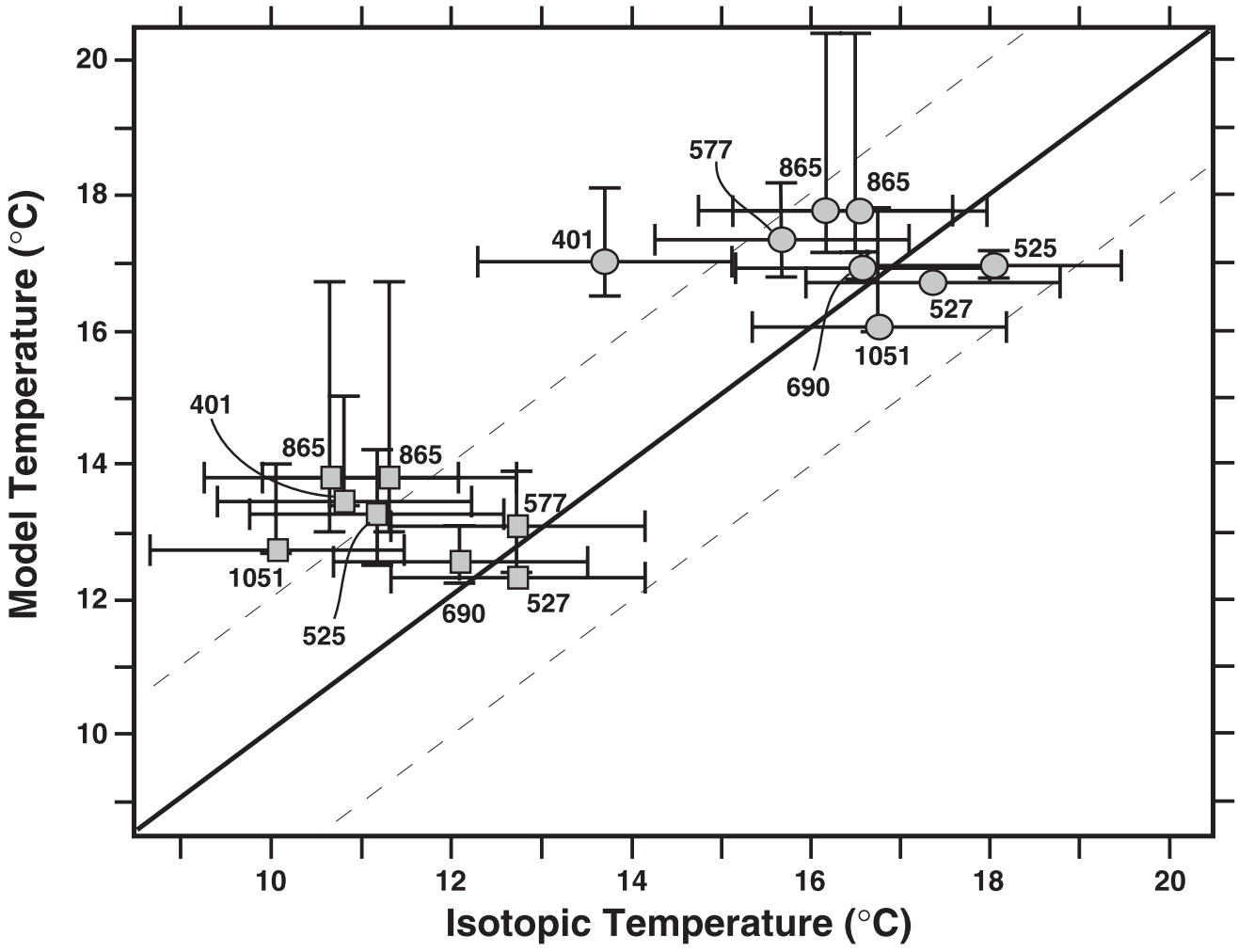

Figure 8. Comparison of model-predicted temperatures and benthic isotopic paleotemperatures for pre-PETM (squares) and PETM (circles) cases. The thick solid line indicates a 1:1 correspondence. Dashed lines indicate the approximate error (±2°C) in the isotopic paleotemperature equation. Error bars are explained in the text. Numbers correspond to ODP and DSDP sites (Table 1).

listed in Table 1. In order to have a somewhat larger data set for comparison, data from Deep Sea Drilling Program (DSDP) Sites 401 and 577 are included even though the peak PETM is missing in benthic records from these sites (see Table 1, footnotes b and d). Peak PETM changes are well recorded at Site 1051, but there is evidence for an unconformity immediately prior to and at the onset of the PETM [*Katz et al.*, 1999].

[18] Paleotemperatures are calculated using the equation of *Erez and Luz* [1983]. An average ocean water $\delta^{18}O$ (δ_w) value of −1.0‰ (standard mean ocean water (SMOW)) is assumed [*Shackleton and Kennett*, 1975]. Horizontal error bars in Figure 8 indicate a 2σ uncertainty in bottom water δ_w based on the standard deviation (σ = 0.16‰) of modern values below 1000 m water depth in the Geochemical Ocean Sections Study data set [*GEOSECS*, 1987]. To convert water $\delta^{18}O$ values from SMOW to the PDB scale, −0.27‰ is used [*Hut*, 1987]. We assume no change in δ_w at the PETM. The uncertainty in the isotopic paleotemperature equation is ∼2°C [*Erez and Luz*, 1983; *Bice et al.*, 2000b], indicated by the dashed lines in Figure 8.

[19] In absolute temperatures the model matches both the inferred pre-PETM and PETM bottom water temperatures to within 3°C at all sites (Figure 8). The temperature change simulated by the model when the THC switch occurs is therefore very similar to changes in water temperature inferred from benthic foraminiferal $\delta^{18}O$ at these sites. However, there are several sources of possible error in the temperature comparison. First, there is likely error in paleodepth reconstructions that can be difficult to quantify. To account for this possible problem when extracting model-predicted temperatures at each site, vertical error bars in Figure 8 indicate the effect of ±500 m error in paleodepth reconstructions. Deeper paleodepths have no effect or would improve the model-data fit. Shallower paleodepths increase the model temperature by 0°−3°C and would worsen the model-data fit for some sites. Secondly, possible interspecies isotopic offsets may exist owing to disequilibrium fractionation of oxygen isotopes. For this reason, we have avoided making direct interspecies comparisons. However, because we compare all isotopic temperatures to those predicted by the model, we make an indirect comparison across species. Published estimates of the isotopic offset between *Cibicidoides* and *Nuttallides* vary within a relatively narrow range of <0.2‰ [*Shackleton et al.*, 1984; *Katz and Miller*, 1991; *Pak an'd Miller*, 1992], but estimated offsets between *Oridorsalis* and *Nuttallides* vary by at least 1.2‰ [*Shackleton et al.*, 1984; *Charisi and Schmitz*, 1996]. Work by

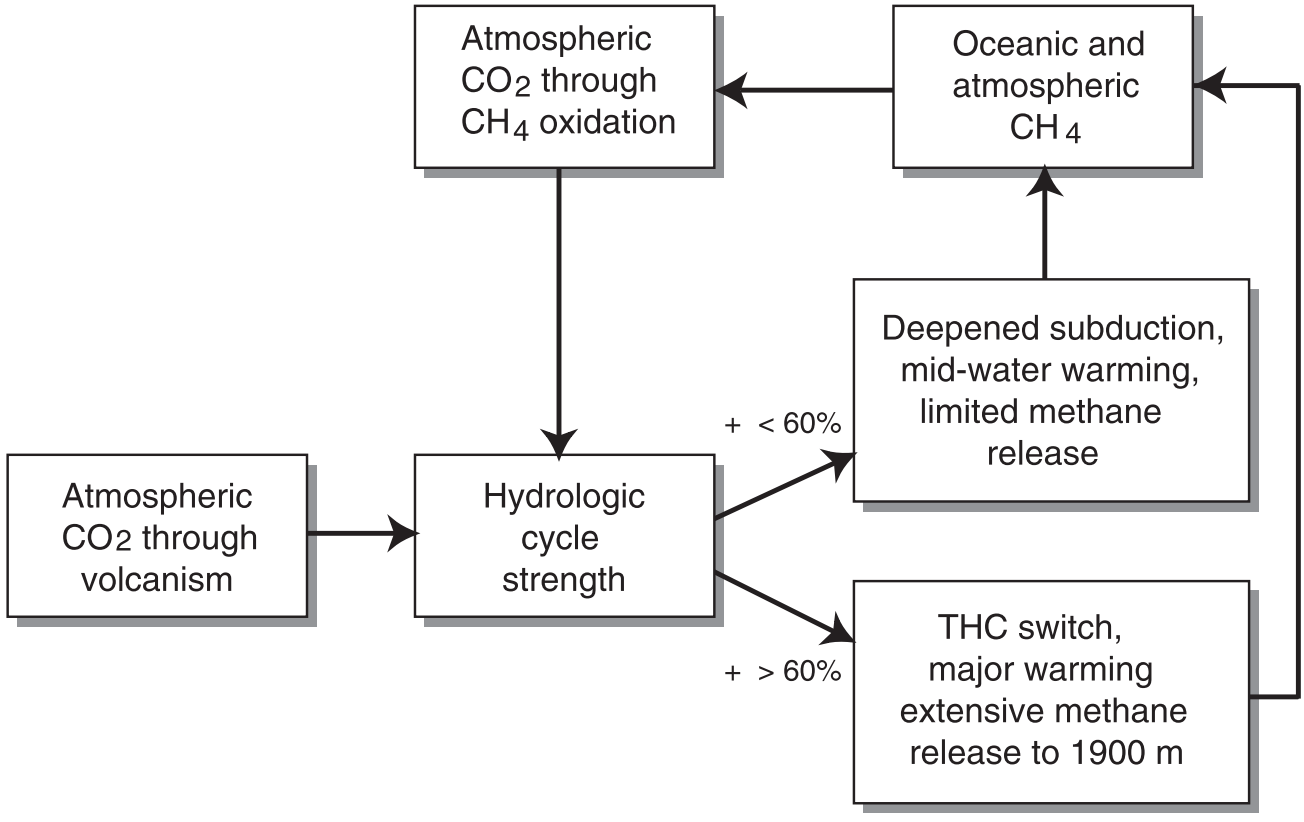

Figure 9. Hypothesized PETM feedback.

M. E. Katz et al. (Paleocene-Eocene benthic foraminiferal isotopes: Species reliability and interspecies correction factors, submitted to *Paleoceanography*, 2001) should produce a consistent set of correction factors for all species used in this study. Until such data are available, we use uncorrected carbonate $\delta^{18}O$ values in the paleotemperature calculations.

[20] As noted in section 2.1, a reasonable fit between model high-latitude sea surface temperatures and those estimated from latest Paleocene planktonic data was achieved by tuning the AGCM greenhouse gas concentrations and slab ocean heat transport coefficient in the atmospheric model from which ocean model forcings were derived. However, we do not compare model surface temperatures and those inferred from $\delta^{18}O$ of pre-PETM and peak PETM planktonic foraminifera because several factors present much greater uncertainty in this comparison: (1) fewer published planktonic data across the event, (2) uncertainty in the depth habitat of planktonic forams, (3) considerable uncertainty in the isotopic composition of ambient seawater and possible changes in this value across the PETM, and (4) uncertainty in tropical sea surface temperatures due to possible early diagenesis [*Pearson et al.*, 2001].

4. Proposed Feedback for the Paleocene-Eocene Thermal Maximum

[21] The abrupt nature of the PETM bottom warming has long been interpreted as indicative of a THC switch, but the switch has been hypothesized to be from high southern latitude sinking to subtropical sinking [*Kennett and Stott*, 1991]. Our results suggest that the abrupt warming may instead have resulted from a switch from high southern to high northern latitude sinking at some critical point in the strength of the hydrologic cycle. This south-north switch in thermohaline circulation may therefore represent the "threshold" ocean response invoked for the PETM [*Kennett and Stott*, 1991; *Zachos et al.*, 1993; *Dickens et al.*, 1995].

[22] We propose a positive feedback (Figure 9) in which an increase in the strength of the hydrologic cycle (perhaps initiated by volcanic outgassing of CO_2) leads first to subduction warming at intermediate depths and spatially limited thermal hydrate destabilization. Some part of the methane thus released is oxidized to CO_2 in either the ocean or atmosphere [*Dickens*, 2000]. We hypothesize that increased atmospheric concentrations of CO_2 (and plausibly methane) would further amplify the hydrologic cycle increase, eventually causing an abrupt switch to sinking in the warmer Northern Hemisphere. The resulting widespread, abrupt bottom warming would plausibly result in widespread methane hydrate destabilization as deep as 1900 m water depth over most of the world ocean (Figure 10). The model temperature response to a THC switch suggests that destabilization of hydrates as deep as 2400 m could occur in the entire Northern Hemisphere Pacific basin and a small region of the northeastern North Atlantic. Following the warming associated with a THC switch, bottom water temperatures low enough to support stable hydrates shallower than 1900 m water depth are found only in the high-latitude Pacific sector Southern Ocean.

[23] Limited subduction-induced warming followed by abrupt, widespread warming caused by a switch in thermohaline circulation would allow for sequential, or pulsed, injections of methane carbon, consistent with observations in high-resolution records [*Bains et al.*, 1999; *Röhl et al.*, 2000]. Furthermore, the chain of events is also self-limiting with regard to methane release as the widespread destabilization caused by abrupt deep-ocean warming

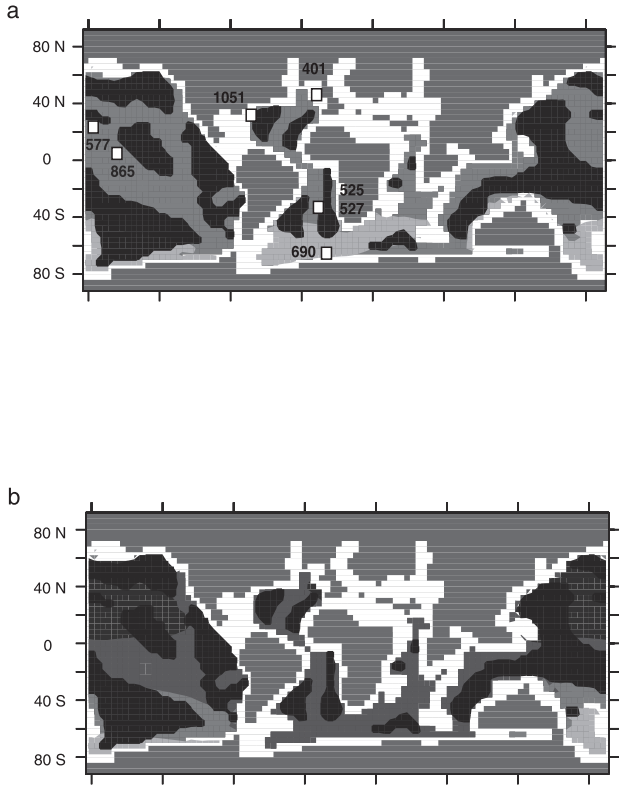

Figure 10. Distribution of possible stable hydrates (a) before and (b) after the THC switch based on model water depth, temperature, and the hydrate stability phase diagram of *Dickens et al.* [1995]. Land areas are shown in gray. White areas indicate bottom water temperatures too warm for stable gas hydrate. Green, stable hydrate at >1100 m depth; blue, >1500 m; red, >1900 m; yellow, >2400 m. Black areas indicate water depths >4000 m where hydrates are unlikely, assuming 4000 m depth for the base of gas hydrate stability [*Dickens et al.*, 1995; *Dickens*, 2001]. Figure 10a is based on temperatures from the 1 $E-P$ case. Figure 10b is from the 1.6 $E-P$ case following the THC switch. Benthic data sites listed in Table 1 are shown in Figure 10a. See color version of this figure at back of this issue.

at the THC switch could occur only once because circulation can not switch again to warm bottom waters further.

5. Predictions of the Hypothesis

[24] The proposed feedback mechanism suggested by the model results has a number of features that should be testable as more PETM sections, especially high-resolution sections, become available. We offer the following general predictions.

1. Gradual surface warming would accompany (and drive) an increase in the hydrologic cycle. Next, thermocline and upper intermediate depths would warm gradually in some areas owing to deepened subduction. Finally, abyssal waters warm abruptly everywhere owing to the THC switch. Thus the PETM and interval immediately preceding it should exhibit a largely "top-down" warming. Whether or not both warming mechanisms would drive destabilization of gas hydrates depends largely on the distribution of hydrates in the depth range of subduction warming (no deeper than 1500 m). *Röhl et al.* [2000] interpret the high-resolution record from Site 1051 as indicating both gradual and catastrophic inputs of isotopically depleted carbon to the ocean system. This is consistent with our prediction of two mechanisms for hydrate destabilization, operating on different timescales.

2. Prior to the massive input of light carbon at the PETM, destabilization of hydrates due to deepened subduction would have occurred at progressively greater depths. This progressive response could have been smooth or pulsed, depending on the true rate of change in atmospheric moisture transports and the location of significant clathrate reservoirs relative to regions of maximum warming.

3. Subduction-induced warming would have been greatest in the Atlantic basins (Figures 7b and 7e). This suggests that it is most likely that destabilization of the shallowest late Paleocene gas hydrates would have occurred in the Atlantic, if subduction indeed drove hydrate melting. While warming caused by the THC switch would be sufficient to destabilize hydrates as deep as 1900 m water depth over the entire Atlantic basin, destabilization at even greater depths (to 2400 m) could have occurred in the Northern Hemisphere Pacific basin but in only a limited region of the northeastern North Atlantic basin. Evidence of PETM calcium carbonate dissolution (assumed to be an indicator of decreased local carbonate ion concentration due to CH_4 oxidation) is apparently most pronounced in the Atlantic Ocean [*Thomas*, 1998]. This lends support to the idea that extensive methane release occurred in the Atlantic [*Katz et al.*, 1999; *Dickens*, 2000]. The model indicates, however, that temperature change associated with the switch to north Pacific bottom water formation would have been sufficient to drive extensive destabilization in that basin as well.

4. The THC should return to Southern Hemisphere deep water formation as radiative gases input to the atmosphere before and during the PETM are removed by long- and short-term carbon cycle processes [*Bains et al.*, 2000; *Beerling*, 2000; *Ravizza et al.*, 2001]. When we decrease $E-P$ from its maximum value of 2.0 to the initial profile, the ocean cools, first gradually as subduction shallows, then abruptly when the THC returns to its original state with deep sinking in the Southern Hemisphere. This cooling, driven by a hydrologic cycle "spin down," is consistent with observations showing that benthic $\delta^{18}O$ values (indicating temperature) decreased to near pre-PETM values over <100 kyr [*Röhl et al.*, 2000]. The model switchback to the original THC state occurs at a lower $E-P$ (1.2 times control) than does the forward switch (1.6 times control), indicating multiple equilibria in a small parameter range for paleogeographies with a Brito-Arctic bridge.

6. Discussion

[25] If the PETM included a switch in thermohaline circulation and massive methane release, why did the event occur at this time? Our results indicate a strong sensitivity to North Atlantic tectonism: the THC switch and subsequent widespread bottom warming occur always and only when a barrier representing possible Greenland-Iceland-Faeroe Ridge uplift is specified in the model configuration. This suggests that the Paleocene-Eocene paleogeography played a critical role in the response of the ocean system to a gradual perturbation of the atmospheric hydrologic cycle. It may be interpreted as a measure for how many influences must conspire, even in a warm climate, to produce an event as remarkable as the PETM. Still, we caution that substantial uncertainties exist in the exact details of the Paleocene/Eocene ocean configuration. With any ocean model, it is necessary to explore the sensitivity of the model solution to fundamental uncertainty in this boundary condition, but it is impossible to test all possible configurations. Similarly, as noted in section 2.1, there exist different combinations of AGCM parameters that can produce nearly the same fit to the initial (pre-PETM) sea surface temperature data on which we have imposed a hydrologic cycle increase, but it is impractical to define

and test the ocean model with all possible combinations. We therefore offer these results as representative of one part of the spectrum of possible THC solutions and sensitivity for the Paleocene-Eocene ocean, with the caveat that we do not know yet if the surface conditions resulting from all possible AGCM combinations of greenhouse gas concentrations and heat transport coefficients would result in a switch in thermohaline circulation.

[26] The model runs shown here have employed some significant idealizations, such as the use of zonal mean atmospheric boundary conditions or the absence of an explicit atmospheric model. While either simplification is expected to change the results quantitatively, we argue that qualitatively, the results are robust. The existence of and transitions between multiple equilibria of the thermohaline circulation is a robust phenomenon, across the range of simple and complex, coupled and uncoupled models [e.g., *Manabe and Stouffer*, 1988; *Marotzke*, 1990; *Marotzke and Willebrand*, 1991; *Weaver and Hughes*, 1992]. In mathematical terms the bifurcation structures of coupled and uncoupled models of the THC are very similar [*Marotzke*, 1996]. Using an uncoupled model might introduce quantitative differences, but it is unlikely to "get things wrong" qualitatively. The justification of a simple model approach is discussed further by *Bice and Marotzke* [2001].

[27] Although we impose a zonal mean forcing to the ocean model, in reality, there is certainly west-east asymmetry in the atmospheric hydrologic cycle, with generally drier conditions over the eastern subtropical oceans [*Peixoto and Oort*, 1992]. This asymmetry is apparent in PETM records from subtropical latitudes of the North Atlantic. *Gibson et al.* [2000] describe clay mineral changes in the Salisbury Embayment (Virginia-New Jersey coastal plain) that suggest an increase in drainage basin-integrated moisture flux over some part of eastern North America. At the same time, PETM drying is supported by mineralogical and isotopic studies in the subtropical eastern North Atlantic and western Europe [*Schmitz et al.*, 2001; *Schmitz and Andreasson*, 2001]. The Salisbury embayment record suggests that western North Atlantic embayment surface waters could have become less saline due to increased runoff during the PETM, but it is unlikely that such a change would have prevented deepened subduction in the North Atlantic. This is because the subduction process that transports warmer, saline water into the thermocline tends to remove surface water from the eastern side of the subtropical gyre and deposit it in the western deep thermocline [*Price*, 2001]. The decreased salinity waters inferred by Gibson et al. may therefore have existed as a lower-density mass in the subtropical marginal western North Atlantic and may have had little influence on thermocline ventilation by subduction.

[28] How literally should we read the fact that in experiments where a THC switch occurred, it occurred at a 60% increase in the strength of the hydrologic cycle? Given the use of zonal mean forcings and the lack of an ocean-atmosphere feedback in the uncoupled model, we would argue only that if such a switch occurred, it occurred at "some critical value" of moisture transport. For example, additional sensitivity experiments were performed in which $E-P$ was increased from a factor of 1.5 at the slower rate of 1% per 500 years. Here the abrupt THC switch occurred at a factor of 1.65 times the control $E-P$, revealing a rate dependence in the model response. The long-term isotopic record indicates that late Paleocene oceans were warming slowly over several million years preceding the PETM [*Zachos et al.*, 2001], and so our hydrologic cycle forcing may be much faster than the actual rate of perturbation of the climate system. It would be impractical to perform experiments of several million years duration using a three-dimensional ocean model. However, we note that the THC response obtained is much faster than the change in forcing, which is the hallmark of an abrupt climate change event [*National Research Council (NRC)*, 2002]. We also note that while an increase in the hydrologic cycle may have begun several million years prior to the PETM event, our sensitivity tests suggest that the THC switch occurs only when a land bridge is present in the North Atlantic. From North American mammalian data we know that the land bridge existed precisely at the time of the PETM. It is not clear from tectonic, faunal, or sedimentary evidence exactly how long the bridge had been in existence prior to the PETM. Regardless of how long the period of time over which the hydrologic cycle increase occurred, the model suggests that the switch might not have occurred until formation of the land bridge.

[29] Climate models, both coupled and uncoupled, differ in their prediction of the magnitude and rate of increase in the water cycle given some increasing CO_2 scenarios [*Manabe et al.*, 1994], and few studies have examined CH_4-induced changes in the hydrologic cycle. How strong the positive feedback in our hypothesized system is would have to be investigated using reliable coupled physical-chemical atmosphere-ocean models. Strict quantification of forcings and feedbacks in such a system is probably not feasible with existing coupled models, given that such models being used for future climate change research do not agree on the fundamental question of whether a future doubling of atmospheric CO_2 will stabilize or destabilize the modern thermohaline circulation [*Manabe and Stouffer*, 1993; *Rahmstorf and Ganopolski*, 1999; *Latif et al.*, 2000].

[30] The precise location and amount of PETM methane release resulting from gradual subduction warming and abrupt THC switch-induced warming are difficult to predict. The many complexities of late Paleocene marine productivity, hydrate formation and stability, sediment stability, and controls on hydrate phase change under gradual and abrupt warming in already "warm" oceans remain to be sorted out by the diverse research community studying the Paleocene-Eocene Thermal Maximum. The results presented here raise the intriguing possibility that an abrupt change in thermohaline circulation from southern to northern sinking was an integral part of the PETM and that this change could have resulted from a gradual increase in the water cycle under conditions of late Paleocene volcanism and Paleocene-Eocene paleogeography.

[31] **Acknowledgments.** This material is based upon work supported by the National Science Foundation under grant ATM-9905023 to K.L.B. and under grant ATM-0000545, which supports the Partnership in Modeling Earth System History (PSU/WHOI). The authors benefited from discussions with J. Pedlosky, R. Norris, D. C. Kelly, and J. Scott. We thank J. Dickens, M. Katz, and E. Thomas for helpful comments on versions of the manuscript and L. Peterson for outstanding editorial support. The MOM2 ocean model was developed under the direction of R. Pacanowski at the Geophysical Fluid Dynamics Laboratory. The GENESIS atmospheric model was developed at the National Center for Atmospheric Research by S. Thompson and D. Pollard. The baseline paleogeography was provided by C. Scotese. The GENESIS model was run on the Cray SV1 system at Pennsylvania State University's Environment Computing Facility. Model data visualization was done using Ferret, a freely distributed software package developed by the Thermal Modeling and Analysis Project at NOAA/PMEL. This is WHOI contribution 10580.

References

Bains, S., R. M. Corfield, and R. D. Norris, Mechanisms of climate warming at the end of the Paleocene, *Science*, *285*, 724–727, 1999.

Bains, S., R. D. Norris, R. M. Corfield, and K. L. Faul, Termination of global warmth at the Palaeocene/Eocene boundary through productivity feedback, *Nature*, *407*, 171–174, 2000.

Beck, R. A., A. Sinha, D. W. Burbank, W. J. Sercombe, and A. M. Khan, Climatic, oceanographic, and isotopic consequences of the Paleocene India-Asia collision, in *Late Paleo-*

cene-Early Eocene Climatic and Biotic Events in the Marine and Terrestrial Records, edited by M.-P. Aubry, S. G. Lucas, and W. A. Berggren, pp. 103–117, Columbia Univ. Press, New York, 1998.

Beerling, D. J., Increased terrestrial carbon storage across the Palaeocene-Eocene boundary, *Palaeogeogr. Palaeoclimatol. Palaeoecol.*, *161*, 395–405, 2000.

Bice, K. L., and J. Marotzke, Numerical evidence against reversed thermohaline circulation in the warm Paleocene/Eocene ocean, *J. Geophys. Res.*, *106*, 11,529–11,542, 2001.

Bice, K. L., E. J. Barron, and W. H. Peterson, Reconstruction of realistic early Eocene paleobathymetry and ocean GCM sensitivity to specified basin configuration, in *Tectonic Boundary Conditions for Climate Reconstructions*, edited by T. Crowley and K. Burke, pp. 227–247, Oxford Univ. Press, New York, 1998.

Bice, K. L., C. R. Scotese, D. Seidov, and E. J. Barron, Quantifying the role of geographic change in Cenozoic ocean heat transport using uncoupled atmosphere and ocean models, *Palaeogeogr. Palaeoclimatol. Palaeoecol.*, *161*, 295–310, 2000a.

Bice, K. L., L. C. Sloan, and E. J. Barron, Comparison of early Eocene isotopic paleotemperatures and the three-dimensional OGCM temperature field: The potential for use of model-derived surface water $\delta^{18}O$, in *Warm Climates in Earth History*, edited by B. T. Huber, K. G. MacLeod, and S. L. Wing, pp. 79–131, Cambridge Univ. Press, New York, 2000b.

Boulter, M. C., and S. B. Manum, The Brito-Arctic igneous province flora around the Paleocene/Eocene boundary, *Proc. Ocean Drill. Program Sci. Results*, *104*, 663–680, 1989.

Bralower, T. J., D. J. Thomas, J. C. Zachos, M. M. Hirschmann, U. Roehl, H. Sigurdsson, E. Thomas, and D. L. Whitney, High-resolution records of the late Paleocene thermal maximum and circum-Caribbean volcanism: Is there a causal link?, *Geology*, *25*, 963–966, 1997.

Bryan, F., High-latitude salinity effects and interhemispheric thermohaline circulations, *Nature*, *323*, 301–304, 1986.

Chamberlin, T. C., On a possible reversal of deep-sea circulation and its influence on geologic climates, *J. Geol.*, *14*, 363–373, 1906.

Charisi, S. D., and B. Schmitz, Early Eocene palaeoceanography and palaeoclimatology of the eastern North Atlantic: Stable isotope results for DSDP Hole 550, in *Correlation of the Early Paleogene in Northwest Europe*, *Geol. Soc. Spec. Publ., 101*, 457–472, 1996.

Clift, P. D., and J. Turner, Paleogene igneous underplating and subsidence anomalies in the Rockall-Faeroe-Shetland area, *Mar. Petrol. Geol.*, *15*, 223–243, 1998.

Clift, P. D., J. Turner, and Leg 152 Scientific Party, The tectonics of volcanic margin formation in the NE Atlantic and the influence of the Icelandic hotspot, *J. Geophys. Res.*, *100*, 24,473–24,486, 1995.

Clift, P. D., A. Carter, M. Krol, and E. Kirby, Constraints on India-Eurasia collision in the Arabian Sea region taken from the Indus Group, Ladakh Himalaya, India, in *The Tectonic and Climatic Evolution of the Arabian Sea Region*, edited by P. D. Clift et al., *Geol. Soc. Spec. Publ.*, in press, 2002.

Clyde, W. C., and P. D. Gingerich, Mammalian community response to the latest Paleocene thermal maximum: An isotaphonomic study in the northern Bighorn Basin, Wyoming, *Geology*, *26*, 1011–1014, 1998.

Crowley, T. J., Paleomyths I have known, in *Modeling the Earth's Climate and Its Variability*, edited by R. Holland, S. Joussaume, and F. David, pp. 377–430, Elsevier Sci., New York, 1999.

de Sigoyer, J., V. Chavagnac, I. M. Villa, J. Blichert-Toft, B. Luais, S. Guillot, M. Cosca, and G. Mascle, Dating the Indian continental subduction and collisional thickening in the northwest Himalaya: Multichronology of the Tso Morari eclogites, *Geology*, *28*, 487–490, 2000.

Dickens, G. R., Methane oxidation during the late Palaeocene thermal maximum, *Bull. Geol. Soc. Fr.*, *171*, 37–49, 2000.

Dickens, G. R., The potential volume of oceanic methane hydrates with variable external conditions, *Org. Geochem.*, *32*, 1177–1193, 2001.

Dickens, G. R., J. R. O'Neil, D. K. Rea, and R. M. Owen, Dissociation of oceanic methane hydrate as a cause of the carbon-isotope excursion at the end of the Paleocene, *Paleoceanography*, *10*, 965–971, 1995.

Driscoll, N. W., G. D. Karner, and J. K. Weissel, Stratigraphic and tectonic evolution of Broken Ridge from seismic stratigraphy and Leg 121 drilling, *Proc. Ocean Drill. Program Sci. Results*, *121*, 71–92, 1989.

Eldholm, O., and E. Thomas, Environmental impact of volcanic margin formation, *Earth Planet. Sci. Lett.*, *117*, 319–329, 1993.

Erez, B., and J. Luz, Experimental paleotemperature equation for planktonic foraminifera, *Geochim. Cosmochim. Acta*, *47*, 1025–1031, 1983.

Geochemical Ocean Sections Study (GEOSECS), *Atlantic, Pacific and Indian Ocean Expeditions*, vol. 7, *Shorebased Data and Graphics*, Int. Decade of Ocean Exp., Natl. Sci. Found., Washington, D. C., 1987.

Gibson, T. G., L. M. Bybell, and D. B. Mason, Stratigraphic and climatic implications of clay mineral changes around the Paleocene/Eocene boundary of the northeastern US margin, *Sed. Geol.*, *134*, 65–92, 2000.

Hall, A., and R. J. Stouffer, An abrupt event in a coupled ocean-atmosphere simulation without external forcing, *Nature*, *409*, 171–174, 2001.

Hut, G., Consultants group meeting on stable isotope reference samples for geochemical and hydrological investigations, Rep. to Dir. Gen., Int. At. Energy Agency, Vienna, 42 pp., 1987.

Kaiho, K., et al., Latest Paleocene benthic foraminiferal extinction and environmental changes at Tawanui, New Zealand, *Paleoceanography*, *11*, 447–465, 1996.

Katz, M. E., and K. G. Miller, Early Paleocene benthic foraminiferal assemblages and stable isotopes in the Southern Ocean, *Proc. Ocean Drill. Program Sci. Results*, *114*, 481–499, 1991.

Katz, M., D. K. Pak, G. R. Dickens, and K. G. Miller, The source and fate of massive carbon input during the latest Paleocene thermal maximum, *Science*, *286*, 1531–1533, 1999.

Katz, M., B. S. Cramer, G. S. Mountain, S. Katz, and K. G. Miller, Uncorking the bottle: What triggered the Paleocene/Eocene thermal maximum methane release?, *Paleoceanography*, *16*, 549–562, 2001.

Kennett, J. P., and L. D. Stott, Abrupt deep-sea warming, palaeoceanographic changes and benthic extinctions at the end of the Paleocene, *Nature*, *353*, 225–229, 1991.

Knox, R. W. O'B., The tectonic and volcanic history of the North Atlantic region during the Paleocene-Eocene transition: Implications for NW European and global biotic events, in *Late Paleocene-Early Eocene Climatic and Biotic Events in the Marine and Terrestrial Records*, edited by M.-P. Aubry, S. G. Lucas, and W. A. Berggren, pp. 91–102, Columbia Univ. Press, New York, 1998.

Koch, P. L., J. C. Zachos, and P. D. Gingerich, Correlation between isotope records in marine and continental carbon reservoirs near the Palaeocene/Eocene boundary, *Nature*, *358*, 319–322, 1992.

Koch, P. L., J. C. Zachos, and D. L. Dettman, Stable isotope stratigraphy and paleoclimatology of the Paleogene Bighorn Basin (Wyoming, USA), *Palaeogeogr. Palaeoclimatol. Palaeoecol.*, *115*, 61–89, 1995.

Kvenvolden, K. A., A primer on the geological occurrence of gas hydrate, in *Gas Hydrates: Relevance to World Margin Stability and Climate Change*, edited by J. P. Henriet and J. Mienert, *Geol. Soc. Spec. Publ., 137*, 9–30, 1998.

Latif, M., E. Roeckner, U. Mikolajewicz, and R. Voss, Tropical stabilization of the thermohaline circulation in a greenhouse warming simulation, *J. Clim.*, *13*, 1809–1813, 2000.

Luyten, J. R., J. Pedlosky, and H. Stommel, The ventilated thermocline, *J. Phys. Oceanogr.*, *13*, 292–309, 1983.

Maas, M. C., M. R. L. Anthony, P. D. Gingerich, G. F. Gunnell, and D. W. Krause, Mammalian generic diversity and turnover in the late Paleocene and early Eocene of the Bighorn and Crazy Mountains Basins, Wyoming and Montana (USA), *Palaeogeogr. Palaeoclimatol. Palaeoecol.*, *115*, 181–207, 1995.

Manabe, S., Early development in the study of greenhouse warming: The emergence of climate models, *Ambio*, *26*, 47–51, 1996.

Manabe, S., and K. Bryan, CO_2-induced change in a coupled ocean-atmosphere model and its paleoclimatic implications, *J. Geophys. Res.*, *90*, 1689–1707, 1985.

Manabe, S., and R. J. Stouffer, Two stable equilibria of a coupled ocean-atmosphere model, *J. Clim.*, *1*, 841–866, 1988.

Manabe, S., and R. J. Stouffer, Century-scale effects of increased atmospheric CO_2 on the ocean-atmosphere system, *Nature*, *364*, 215–218, 1993.

Manabe, S., and R. J. Stouffer, Simulation of abrupt climate change induced by freshwater input to the North Atlantic Ocean, *Nature*, *378*, 165–167, 1995.

Manabe, S., R. J. Stouffer, and M. J. Spelman, Response of a coupled ocean-atmosphere model to increasing atmospheric carbon dioxide, *Ambio*, *23*, 44–49, 1994.

Marotzke, J., Instabilities and multiple equilibria of the thermohaline circulation, *Ber. Inst. Meereskunde 194*, Inst. Meereskunde, Kiel, Germany, 1990.

Marotzke, J., Analysis of thermohaline feedbacks, in *Decadal Climate Variability: Dynamics and Predictability*, edited by D. L. T. Anderson and J. Willebrand, pp. 333–378, Springer-Verlag, New York, 1996.

Marotzke, J., and J. Willebrand, Multiple equilibria of the global thermohaline circulation, *J. Phys. Oceanogr.*, *21*, 1372–1385, 1991.

Matsumoto, R., Causes of the $\delta^{13}C$ anomalies of carbonates and a new paradigm "Gas Hydrate Hypothesis", *J. Geol. Soc. Jpn.*, *11*, 902–924, 1995.

National Research Council (NRC), *Abrupt Cli-*

mate Change: Inevitable Surprises, National Academy of Sciences, Washington, D.C., in press, 2002.

Pacanowski, R., MOM 2 documentation: Users guide and reference manual, *Ocean Tech. Rep. 3.2*, Geophys. Fluid Dyn. Lab, Princeton, N. J., 1996.

Pak, D. K., and K. G. Miller, Paleocene to Eocene benthic foraminiferal isotopes and assemblages: Implications for deepwater circulation, *Paleoceanography*, *7*, 405–422, 1992.

Pearson, P. N., P. W. Ditchfield, J. Singano, K. G. Harcourt-Brown, C. J. Nicholas, R. K. Olsson, N. J. Shackleton, and M. A. Hall, Warm tropical sea surface temperatures in the late Cretaceous and Eocene epochs, *Nature*, *413*, 481–487, 2001.

Peirce, J., J. Weissel, and Leg 121 Scientific Party, Site 757, *Proc. Ocean Drill. Program Sci. Results*, *121*, 305–358, 1989.

Peixoto, J. P., and A. H. Oort, *Physics of Climate*, 520 pp., Am. Inst. of Phys., New York, 1992.

Price, J. F., Subduction, in *Ocean Circulation and Climate: Observing and Modelling the Global Ocean*, edited by G. Siedler, J. Church, and J. Gould, pp. 357–371, Academic, San Diego, 2001.

Quilty, P. G., Upper Cretaceous benthic foraminifers and paleoenvironments, southern Kerguelen Plateau, Indian Ocean, *Proc. Ocean Drill. Program Sci. Results*, *120*, 393–443, 1992.

Rahmstorf, S., and A. Ganopolski, Long-term global warming scenarios computed with an efficient coupled climate model, *Clim. Change*, *43*, 353–367, 1999.

Ravizza, G., R. N. Norris, J. Blusztajn, and M.-P. Aubry, An osmium isotope excursion associated with the late Paleocene thermal maximum: Evidence of intensified chemical weathering, *Paleoceanography*, *16*, 155–163, 2001.

Ritchie, J. D., and K. Hitchen, Early Paleogene offshore igneous activity to the northwest of the UK and its relationship to the North Atlantic igneous province, in *Correlation of the Early Paleogene in Northwest Europe*, *Geol. Soc. Spec. Publ., 101*, 63–78, 1996.

Robert, C., and J. P. Kennett, Antarctic subtropical humid episode at the Paleocene-Eocene boundary: Clay-mineral evidence, *Geology*, *22*, 211–214, 1994.

Roberts, D. G., J. Backman, A. C. Morton, J. W. Murray, and J. B. Keene, Evolution of volcanic rifted margins: Synthesis of Leg 81 results on the west margin of Rockall Plateau, *Deep Sea Drill. Project Initial Rep.*, *81*, 883–912, 1984.

Röhl, U., T. J. Bralower, R. D. Norris, and G. Wefer, New chronology for the late Paleocene thermal maximum and its environmental implications, *Geology*, *28*, 927–930, 2000.

Schmitz, B., and F. P. Andreasson, Air humidity and lake $\delta^{18}O$ during the latest Paleocene-earliest Eocene in France from recent and fossil fresh-water and marine gastropod $\delta^{18}O$, $\delta^{13}C$, and $^{87}Sr/^{86}Sr$, *Geol. Soc. Am. Bull.*, *113*, 774–789, 2001.

Schmitz, B., V. Pujalte, and K. Núñez-Betelu, Climate and sea-level perturbations during the initial Eocene thermal maximum: Evidence from siliciclastic units in the Basque Basin (Ermua, Zumaia and Trabakua Pass), northern Spain, *Palaeogeogr. Palaeoclimatol. Palaeoecol.*, *165*, 299–320, 2001.

Shackleton, N. J., and J. P. Kennett, Paleotemperature history of the Cenozoic and the initiation of Antarctic glaciation: Oxygen and carbon isotope analyses in DSDP Sites 277, 279, and 281, *Deep Sea Drill. Project Initial Rep.*, *29*, 743–755, 1975.

Shackleton, N. J., M. A. Hall, and A. Boersma, Oxygen and carbon isotope data from Leg 74 foraminifers, *Deep Sea Drill. Project Initial Rep.*, *74*, 599–612, 1984.

Stott, L. D., J. P. Kennett, N. J. Shackleton, and R. M. Corfield, The evolution of Antarctic surface waters during the Paleogene: Inferences from the stable isotopic composition of planktonic foraminifers, ODP Leg 113, *Proc. Ocean Drill. Program Sci. Results*, *113*, 849–863, 1990.

Thomas, E., Biogeography of the late Palaeocene benthic foraminiferal extinction, in *Late Paleocene-Early Eocene Climatic and Biotic Events in the Marine and Terrestrial Records*, edited by M.-P. Aubry, S. G. Lucas, and W. A. Berggren, pp. 214–243, Columbia Univ. Press, New York, 1998.

Thomas, E., and N. J. Shackleton, The Paleocene-Eocene benthic foraminiferal extinction and stable isotope anomalies, in *Correlation of the Early Paleogene in Northwest Europe*, *Geol. Soc. Spec. Publ., 101*, 401–441, 1996.

Thomas, E., J. C. Zachos, and T. J. Bralower, Deep sea environments on a warm Earth: Latest Paleocene-early Eocene, in *Warm Climates in Earth History*, edited by B. T. Huber, K. G. MacLeod, and S. L. Wing, pp. 132–160, Cambridge Univ. Press, New York, 2000.

Thompson, S. L., and D. Pollard, Greenland and Antarctic mass balances for present and doubled CO_2 from the GENESIS version 2 global climate model, *J. Clim.*, *10*, 871–900, 1997.

Tiffney, B. H., Wyoming: A crossroads in the Paleogene tropics (abstract), in *Climate and Biota of the Early Paleogene, Abstract Volume*, edited by A. W. Ash and S. L. Wing, p. 94, Smithsonian Inst., Washington, D. C., 2001.

Weaver, A. J., and T. M. C. Hughes, Stability and variability of the thermohaline circulation and its link to climate, in *Trends in Physical Oceanography*, *Research Trends Ser.*, vol. 1, pp. 15–70, Council of Sci. Res. Integration, Trivandrum, India, 1992.

White, N. J., and B. Lovell, Measuring the pulse of a plume with the sedimentary record, *Nature*, *387*, 888–891, 1997.

Zachos, J. C., K. C. Lohmann, J. C. G. Walker, and S. W. Wise, Abrupt climate change and transient climates during the Paleogene—A marine perspective, *J. Geol.*, *101*, 191–213, 1993.

Zachos, J. C., M. Pagani, L. Sloan, E. Thomas, and K. Billups, Trends, rhythms, and aberrations in global climate 65 Ma to present, *Science*, *292*, 686–693, 2001.

K. L. Bice, Department of Geology and Geophysics, Woods Hole Oceanographic Institution, Woods Hole, MA 02543-1541, USA. (kbice@whoi.edu)

J. Marotzke, School of Ocean and Earth Science, Southampton Oceanography Centre, Southampton, SO14 3ZH, UK.

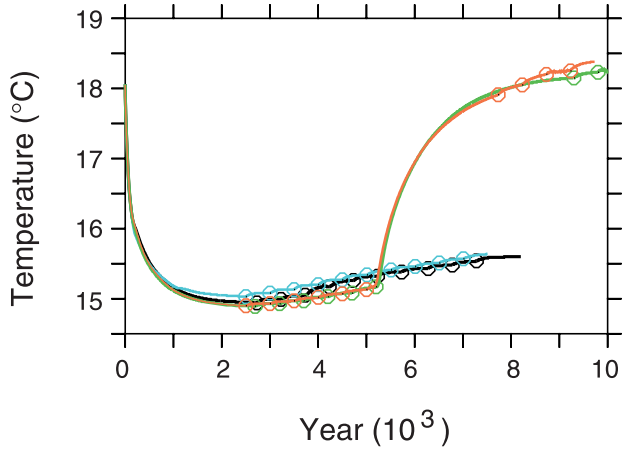

Figure 3. Time series of global mean ocean temperature for the four paleogeography sensitivity tests. The circles indicate the points at which the $E-P$ forcing to the ocean model was increased by 10%. Temperature and wind stress forcings were held constant throughout. Colors indicate the following cases: black, open North Atlantic, open India-Eurasia gateway (Figures 4a and 4c); blue, open North Atlantic, closed India-Eurasia gateway (Figures 4a and 4d); green, Brito-Arctic bridge, closed India-Eurasia gateway (Figures 4b and 4d); red, Brito-Arctic bridge, open India-Eurasia gateway (Figure 4b and 4c).

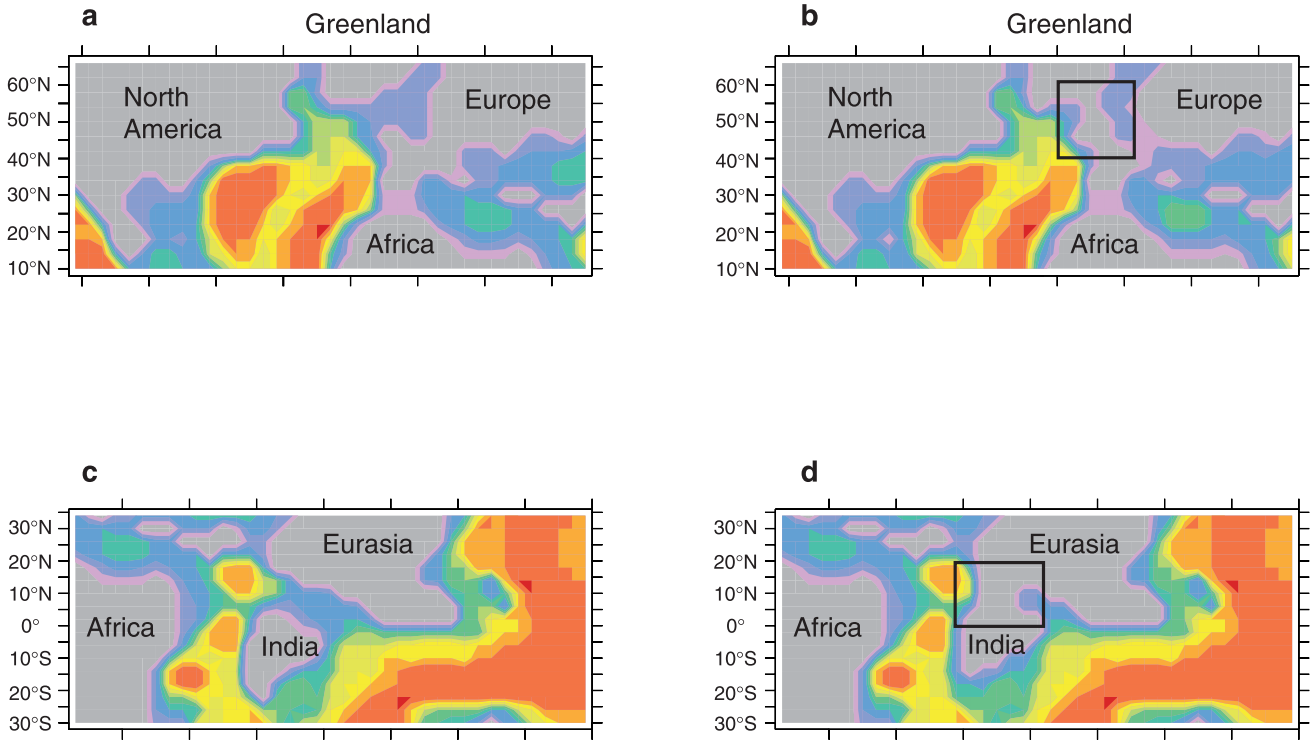

Figure 4. Maps showing regional paleogeographies examined in ocean model sensitivity experiments. (a) Open North Atlantic, (b) Brito-Arctic bridge in the North Atlantic basin, (c) open India-Eurasia gateway, (d) closed India-Eurasia gateway. Gray, land; purple and blues, ocean shallower than 1500 m; orange and reds, ocean deeper than 3000 m.

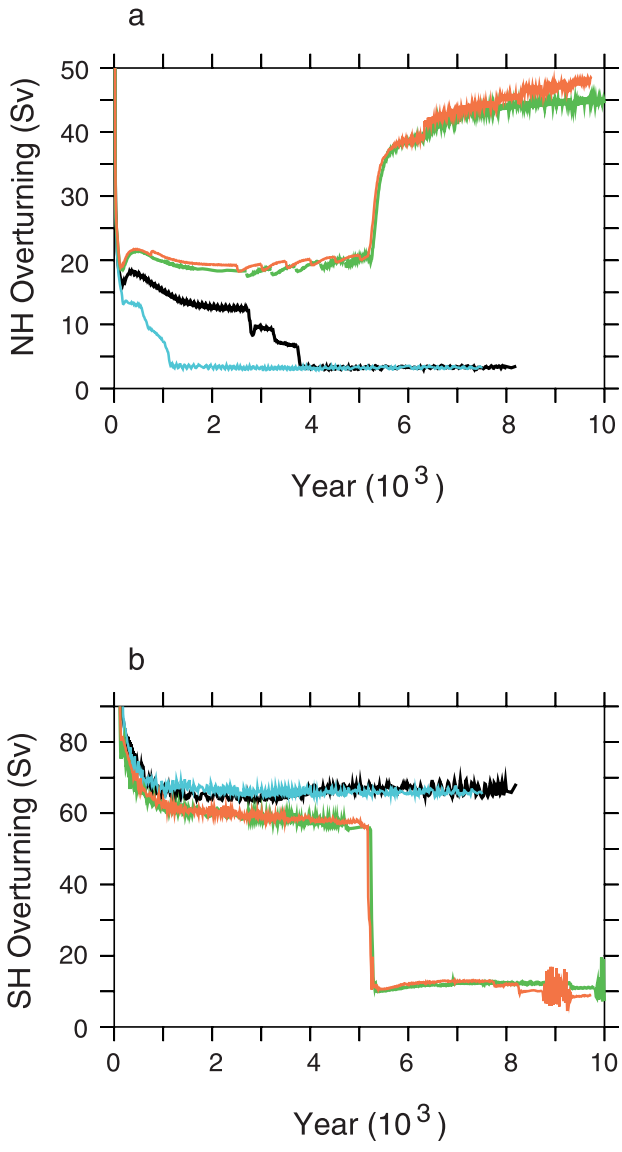

Figure 5. Time series of the maximum meridional overturning strength (Sverdrups) for (a) Northern Hemisphere and (b) Southern Hemisphere. Colors are as indicated for Figure 3.

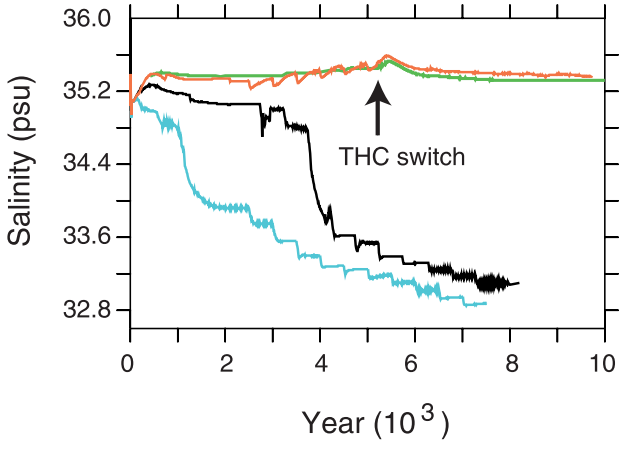

Figure 6. Time series of North Pacific upper ocean salinities in the region of convection, near the Alaskan margin. Colors are as indicated for Figure 3.

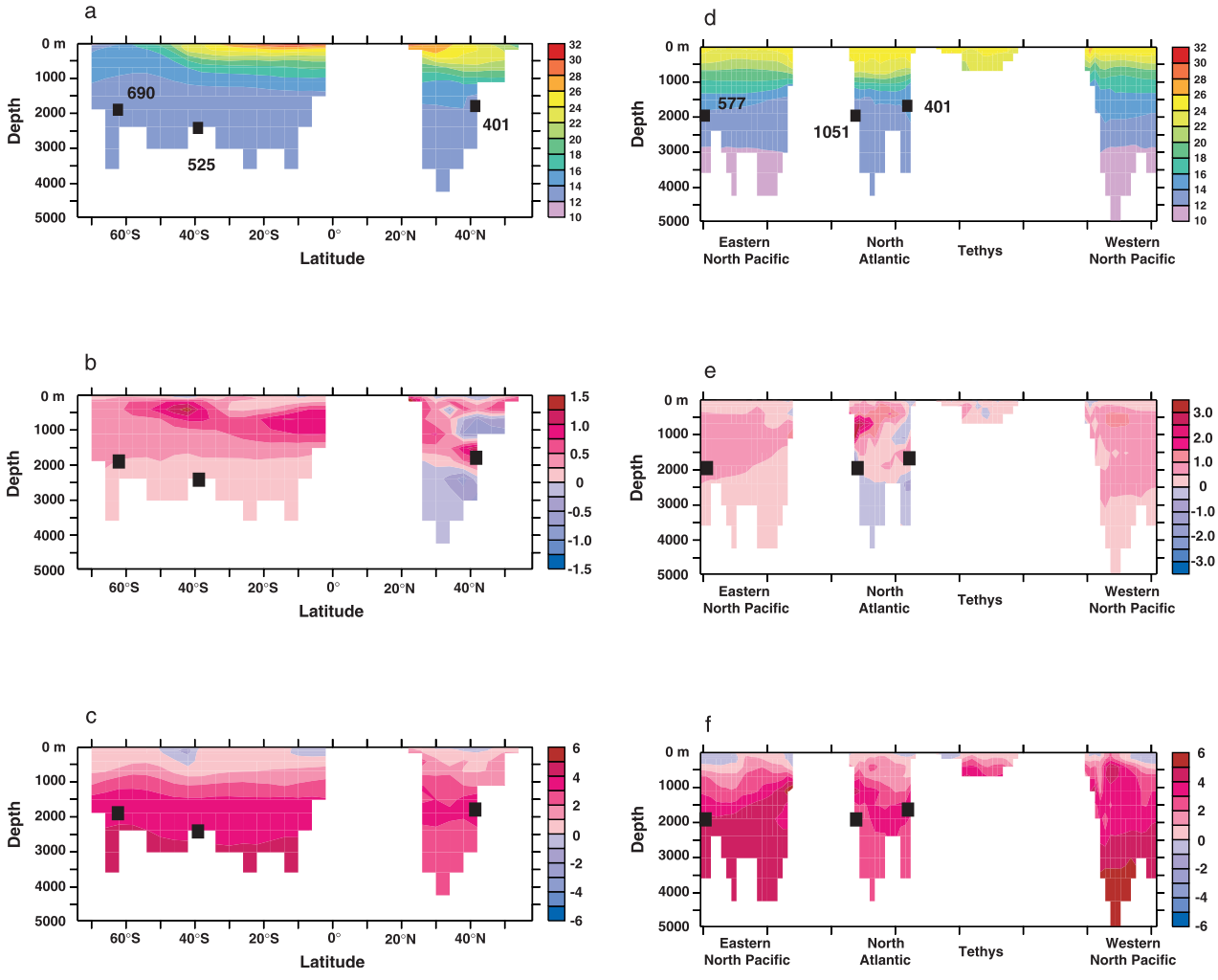

Figure 7. (a–c) Meridional cross sections through the Atlantic basins at the longitude of DSDP Site 401. (d–f) Zonal cross sections near the paleolatitude of Site 401 (38°N). Temperatures from the control case are shown in Figures 7a and 7d. Temperature differences due to deepened subduction are shown in Figures 7b and 7e. Temperature differences due to the THC switch are shown in Figures 7c and 7f. Positive values (reds) indicate warming caused by deepened subduction or by the switch from Southern to Northern Hemisphere bottom water formation.

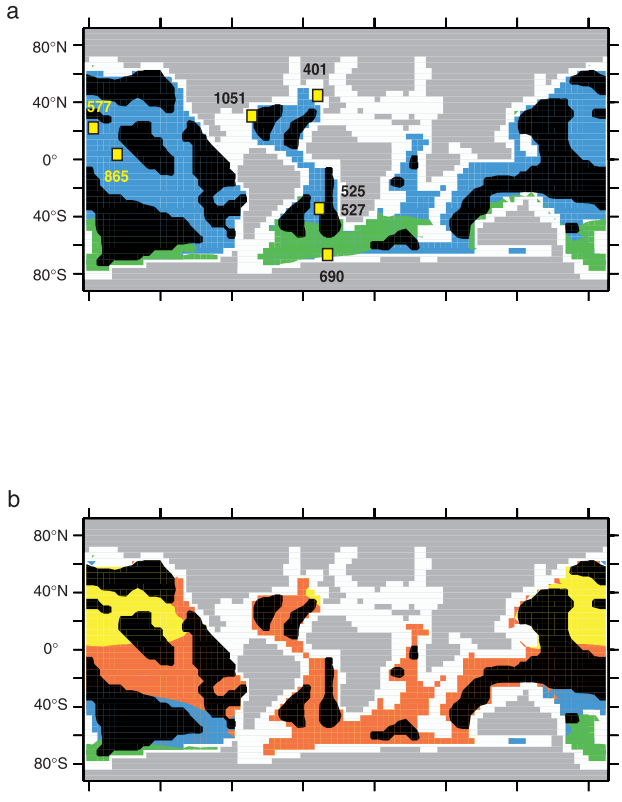

Figure 10. Distribution of possible stable hydrates (a) before and (b) after the THC switch based on model water depth, temperature, and the hydrate stability phase diagram of *Dickens et al.* [1995]. Land areas are shown in gray. White areas indicate bottom water temperatures too warm for stable gas hydrate. Green, stable hydrate at >1100 m depth; blue, >1500 m; red, >1900 m; yellow, >2400 m. Black areas indicate water depths >4000 m where hydrates are unlikely, assuming 4000 m depth for the base of gas hydrate stability [*Dickens et al.*, 1995; *Dickens*, 2001]. Figure 10a is based on temperatures from the 1 $E-P$ case. Figure 10b is from the 1.6 $E-P$ case following the THC switch. Benthic data sites listed in Table 1 are shown in Figure 10a.